COMPARISON OF SAN MARCO ASSI SOLAR EUV AND EUV91 MODEL

W. K. Tobiska,* G. Schmidtke,** H. Doll,*** T. N. Woods,†
J. Worden† and S. Chakrabarti‡

* *TELOS/JPL, MS 264-765, 4800 Oak Grove Drive, Pasadena, CA 91109, U.S.A.*
** *IPM, Heidenhofstrasse 8, D-7800 Freiburg, Germany*
*** *PTS, Leinenweberstrasse 16, D-7800 Freiburg, Germany*
† *HAO/NCAR, P.O. Box 3000, Boulder, CO 80307, U.S.A.*
‡ *Boston University, Center for Space Physics, Boston, MA 02215, U.S.A.*

ABSTRACT

Data from the San Marco-5 Airglow Solar Spectrometer Instrument (ASSI), calibrated to a November 10, 1988 rocket experiment, are compared in absolute values and relative variations with the EUV91 solar irradiance model for up to 38 days in 1988 between days 119 and 316. The calibration of the long-term sensitivity of each of two ASSI spectrometers is analyzed and found to be well-calibrated and self-consistent between similar solar chromospheric wavelengths within each spectrometer. Absolute irradiance values fall within the ±35% uncertainty levels of the model and emission increases due to solar cycle 22 rise are consistent between the data and the model. The internal calibration self-consistency is also investigated with most of the uncertainty in the data variations accounted for by variability within and between the four parameters of wavelength, date of observation, grating, and detector/electronics. Differences between the datasets are not due to solar pointing nor to physical characteristics of the solar emissions. There is still some uncertainty in the calibration of the ASSI datasets with respect to the broad spectral interval over each channel. Whether or not this is a wavelength dependent grating or detector sensitivity change over time remains an open question although there are indications of possible unexplained grating changes toward shorter wavelengths.

INTRODUCTION

The solar extreme ultraviolet (EUV) irradiances from 20 nm to the visible were successfully observed by the ASSI (Schmidtke et al. /1,2/) between March and December 1988. Recent calibration efforts have provided a reference solar spectrum for moderate solar activity based on the ASSI dataset combined with a solar rocket experiment (Woods and Rottman /3/; Schmidtke et al. /4/). As part of this calibration activity, selected wavelengths from the ASSI dataset are compared with irradiances from the EUV91 empirical solar EUV model (Tobiska /5/) for similar levels of solar activity. The results of that comparison and open calibration issues are discussed below. This work extends the preliminary long-term sensitivity analysis by Tobiska et al. /6/.

SAN MARCO ASSI

Schmidtke et al. /1,2,4,7/ describe the ASSI instrument detail and it's preliminary calibration and science results. The instrument consisted of two separate spectrometers, ASSI A & B, covering the wavelength region of 20 nm to the visible with a resolution of about 1 nm in the EUV spectral range up to 110 nm.

The incident radiation entered each spectrometer through a plasma mesh, straylight baffle, and entrance slit before reflecting off a grating which dispersed the light through exit slits and into detectors with their associated electronics. An independent instrument sun-pointing system slightly adjusted the light path to correct for coarse satellite sun-pointing during the semiannual

23° change in the sun's inclination relative to the orbit plane and satellite spin axis. Data points used in this study discussed below were selected only from days where accurate sun-pointing information was available. Figure 1 shows the instrument design for both ASSI A and B.

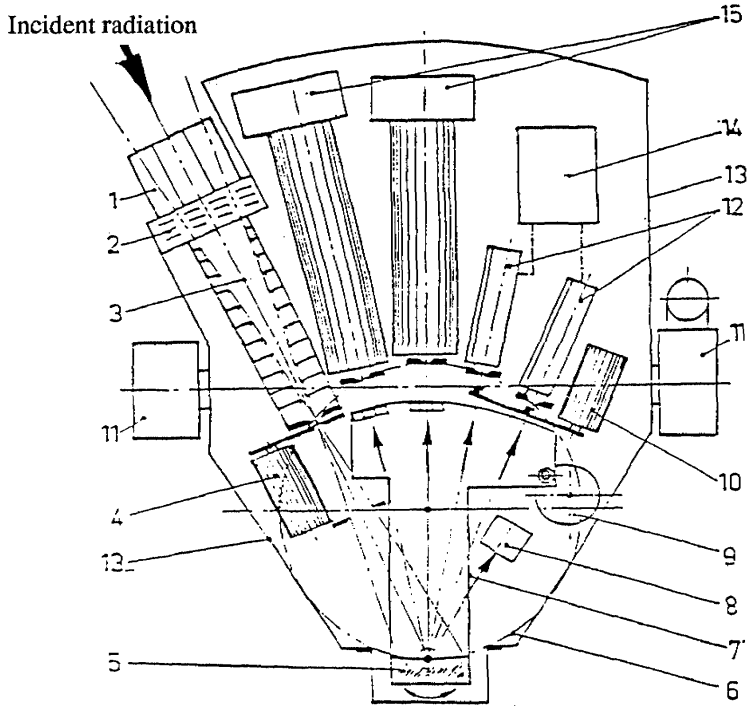

Figure 1. ASSI A and B optical system from Schmidtke et al. /1/. 1 sun sensor, 2 plasma mesh, 3 straylight baffle, 4 mechanics for entrance slits, 5 optical grating, 6 Rowland circle with exit slits, 7 filter wheel mechanics, 8 zero order baffle, 9 driving module, 10 calibration source, 11 sun pointing system, 12 channeltron modules, 13 mechanical structure, 14 charge sensitive amplifiers for 15 multipliers with pre-amplifiers.

Each of the two spectrometers had several channels which were sensitive across a broad range of wavelengths. For example, and of interest below, ASSI A channel 18 (called 11A in Schmidtke et al. /1/) was sensitive between 59 - 140 nm and channel 12 was sensitive between 18 - 98 nm. ASSI B channel 16 was sensitive between 56 -111 nm and channel 17 was sensitive between 4 - 57 nm. Channel is used synonymously with detector and associated electronics. The effective cutoff in overall instrument sensitivity was shortward of 20 nm.

EUV91 MODEL

The EUV91 empirical model extends from 1947 to the present for coronal EUV full-disk irradiances and from 1976 to the present for chromospheric EUV full-disk irradiances. The solar Lyman-α (121.6 nm) and He I 10,830 Å equivalent width (EW) measurements are used as the independent model parameters for the chromospheric irradiances while the 10.7 cm radio flux, $F_{10.7}$, daily and 81-day running mean values are the independent parameters for the coronal and transition region irradiances. The model produces full-disk photon fluxes at 1 AU for 39 EUV wavelength groups and discrete lines between 1.8 and 105.0 nm for a given date. Data from the OSO1/3/4/6, AEROS A, AE-E satellites and six rockets are used in the model development. The irradiances from this model are given as

$$F(\lambda,t) = a_0(\lambda) + \sum_{i=1}^{4} a_i(\lambda)F_i(t) \qquad (1)$$

where $F_i(t)$ (i = 1,2,3,4) are the proxy datasets. For example, $F_1(t)$ is Lyman-α, $F_2(t)$ is He I 10,830 Å EW scaled to Lyman-α values, $F_3(t)$ is daily $F_{10.7}$, and $F_4(t)$ is the 81-day running mean value of $F_{10.7}$. The other coefficients of $a_{i=0-4}(\lambda)$ are tabulated in Tobiska /5/. Missing proxy data are substituted with other proxy data which do exist on given dates through an empirical relationship. Figure 2 shows examples of the model for low, moderate, and high solar activity conditions. Figure 3, adapted from Ogawa et al. /8/, shows a comparison of the model with several rocket flights and two previous models, i.e., those of Donnelly and Pope /9/ and SC#21REFW (Hinteregger et al. /10/), for the 5.0 - 57.5 nm integrated flux wavelength range. Also shown in this figure is the moderate solar activity range of the ASSI observations. The model was run for the entire year of 1988 for this study.

ASSI CALIBRATION

Calibration of the ASSI EUV/UV observations has been a complicated task. There are several calibration components which have been considered by Woods and Rottman /3/, Schmidtke et al. /2/, and Schmidtke et al. /4/. In addition to preflight calibrations, there were on-board radioactive sources for detector and electronics calibration, overlapping spectral regions between channels for inter-channel calibration, and comparison of ASSI flux to the November 10, 1988 LASP rocket EUV spectrum (day 315) and to the SME solar Lyman-α and FUV datasets for absolute intensity calibration. The comparison of ASSI flux to the EUV91 model between 25 and 105 nm for long-term sensitivity calibration is discussed in detail below.

Preliminary conclusions by Woods [private communication, 1992] in regards to the overall variability of the ASSI dataset are that the contrast ratios for both chromospheric and coronal emissions are similar to those derived using AE-E data. Woods also concludes that daily ASSI deviations from simple empirical relationships, i.e., line fits to the ASSI time series, are on the order of 30%. This preliminary conclusion is somewhat larger than the Tobiska et al. /6/ expectation that daily peak-to-valley He II 30.4 nm emissions should be on the order of 11-15%.

A recent product of the calibration process is the presentation of a reference spectrum (Schmidtke et al. /4/). Figure 4 shows that spectrum for moderate solar activity ($F_{10.7}$ ~ 150) with flux binned in 1 nm intervals.

In order to assess the validity of the ASSI calibration, it can be asked how well does the existing calibration account for long-term changes? Does the calibration give reasonable absolute flux and relative variation? Is the calibration internally consistent? Finally, what are the remaining calibration issues? The channels and wavelengths that were selected for comparison of the ASSI data and the EUV91 model were

	ASSI A	ASSI B
channel	12 (55.4 & 85-90 nm)	17 (55.4 & 30.4 nm)
channel	18 (85-90 nm)	16 (85-90 nm)

which allow comparison of high signal-to-noise data from similar solar source regions.

DISCUSSION

Long-term changes in the ASSI dataset and a first order estimate of the calibration of the sensitivity change of the instrument can be seen in the following figures. Figures 5 and 6, panels *a*, *b*, and *c* in each, show the EUV91 modeled solar emissions and the ASSI data compared on an

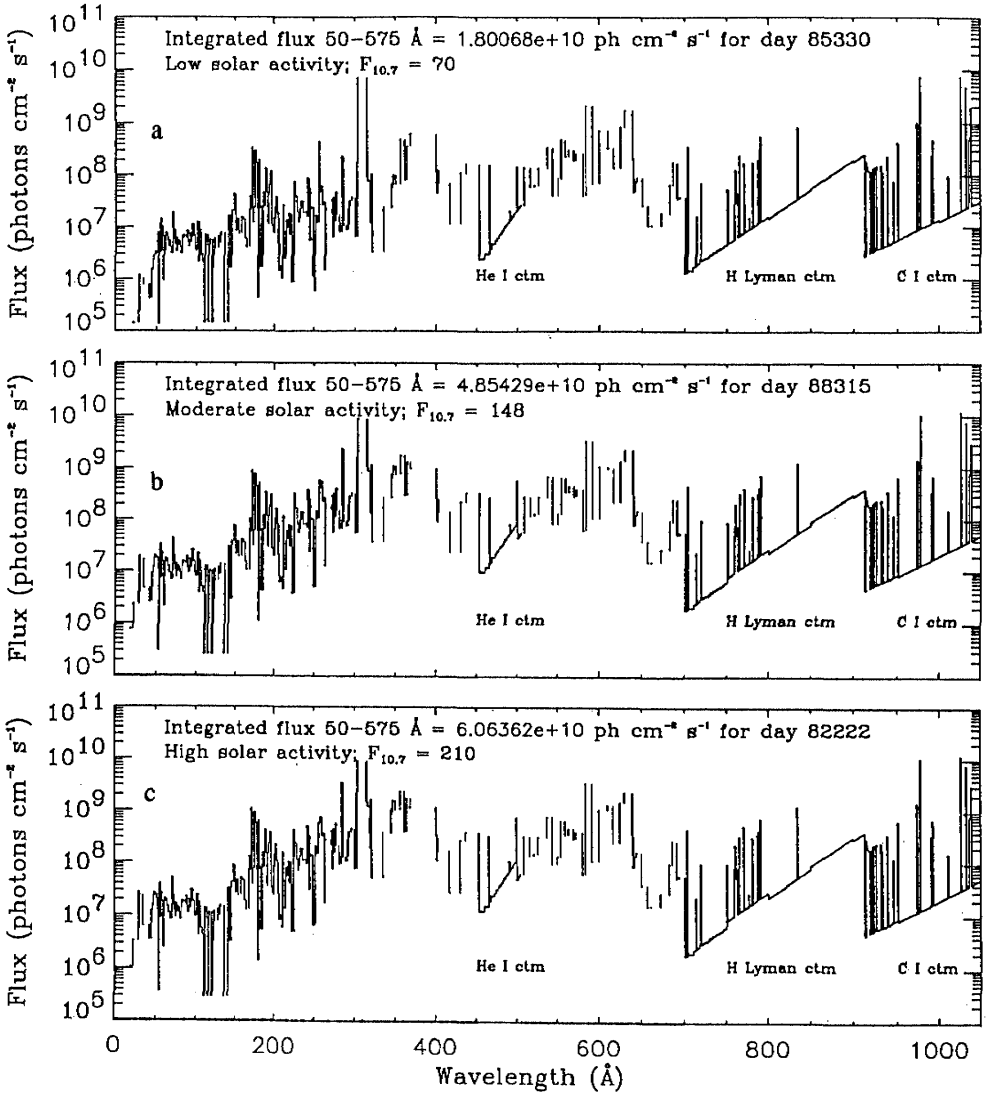

Figure 2. The EUV91 model solar EUV spectrum for November 26, 1985 (low solar activity), for November 10, 1988 (moderate activity), and for August 10, 1982 (high activity) are shown in three panels. The total integrated flux for 5.0 to 57.5 nm is 18.0×10^9 photons cm^{-2} s^{-1} for the November 1985 case, 48.5×10^9 photons cm^{-2} s^{-1} for the November 1988 case, and 60.6×10^9 photons cm^{-2} s^{-1} for the August 1982 case. The He I continuum is visible between 45.0 and 50.4 nm, the H Lyman continuum is between 70.0 and 91.2 nm, and the C I continuum is between 91.3 and 105.0 nm in each panel. Discrete emission lines rise considerably higher than the continua. The modeled spectrum is based on the wavelength ranges of the SC#21REFW spectrum, i.e., mostly 0.1-0.2 nm linewidths, and contains missing lines.

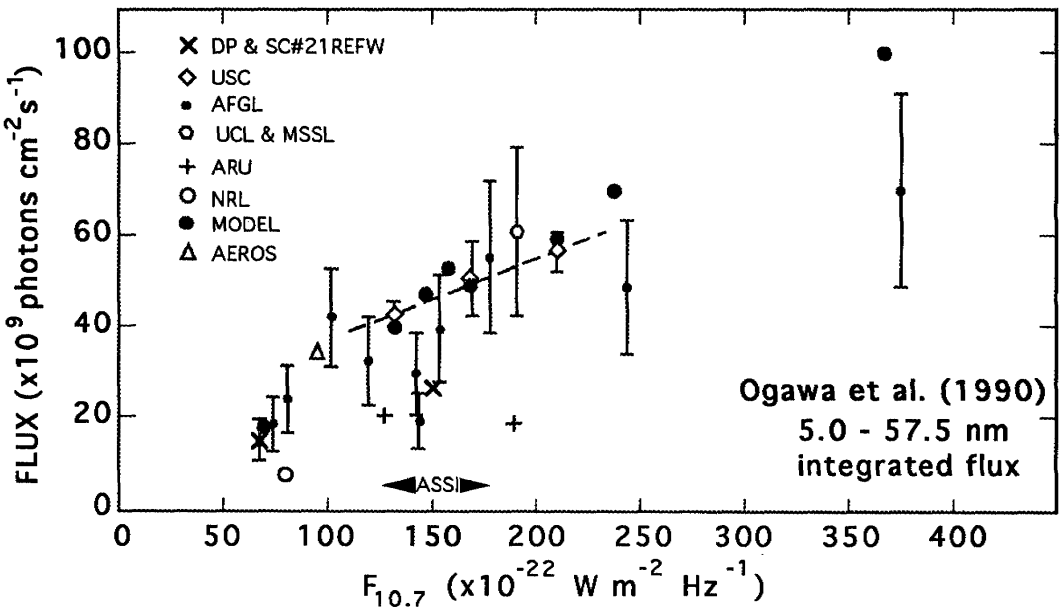

Figure 3. The total integrated solar EUV flux from 5.0 to 57.5 nm adapted from Ogawa et al. /8/. Organizations that made individual rocket measurements are described in that reference. The USC data have the lowest uncertainty and are denoted by diamonds. The model values for a variety of levels of solar activity, as indicated by $F_{10.7}$ in the abscissa, are shown as filled circles with no error bars. Additional data points have been added with the AEROS A satellite measurement on January 19, 1973, when $F_{10.7} = 95$, which had an integrated flux of 34.6×10^9 ±20% described by Schmidtke /11/, the Donnelly and Pope /9/ (DP) integrated flux, and the SC#21REFW /10/ integrated flux. The integrated fluxes for the two latter spectra are 26.9×10^9 ($F_{10.7} = 150$) and 15.0×10^9 ($F_{10.7} = 68$), respectively, and are denoted by an X on the figure.

absolute scale of photon flux versus day of 1988. The model is the dotted line and the data are the boxes connected by a solid line. Corresponding to each data point is a diamond on the model line to enable the reader to visually compare the data and model. In Figure 5*a* the 30.4 nm emission (from ASSI B channel 17) saw a 10% rise in the model and an 11% rise in the data from day 119 to day 316 (25 data points were used). Figure 5*b* shows the 55.4 nm emission (ASSI B channel 17) with a 10% rise in the model and an 11% rise in the data from day 119 to day 316 (12 data points). Figure 5*c* shows the 55.4 nm emission (ASSI A channel 12) with an 11% rise in the model and a 15% rise in the data from day 119 to day 316 (24 data points). The discrepancy between the model 10% and 11% rise in the 5*b* and 5*c* panels 55.4 nm emission is due to linefits through different sets (days) of data points. The absolute flux for all three observed time series is less than the model at the -35% uncertainty level (of the model) as denoted by the error bar centered on day 315.

The conclusions that can be drawn from Figure 5 are that the ASSI B channel 17 (30.4 and 55.4 nm emissions) and the ASSI A channel 12 (55.4 nm emission) are well calibrated for long-term instrument sensitivity changes. The rise in flux levels over a half year are consistent with the rise of solar cycle 22 emission suggested by the model. This also means that ASSI B channel 17 and ASSI A channel 12 are consistent with each other in their long-term sensitivity calibration.

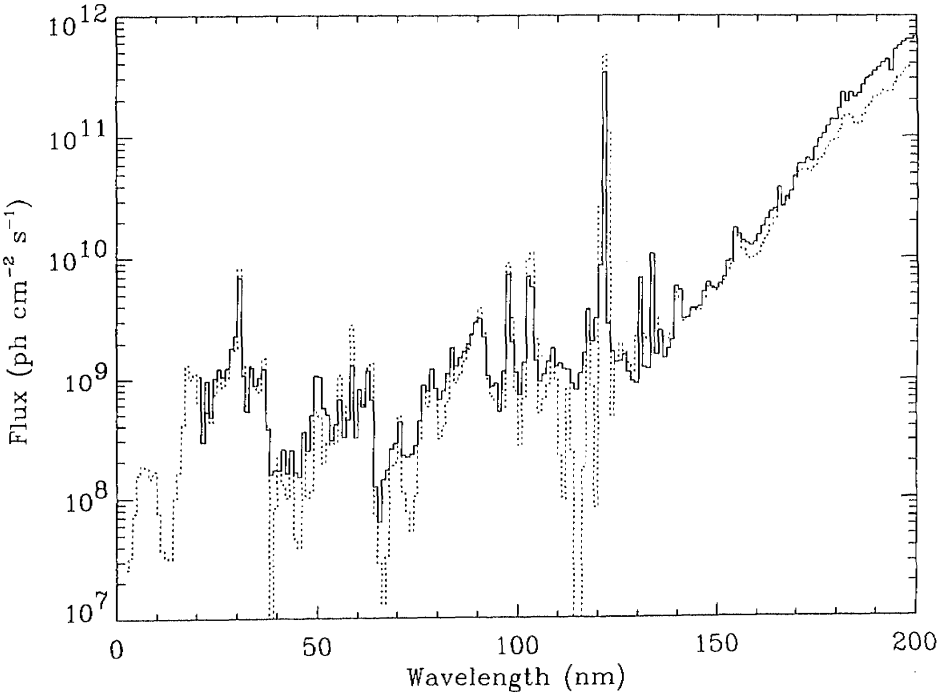

Figure 4. ASSI solar EUV and FUV irradiance spectrum in 1 nm intervals (solid line) compared with modeled EUV flux from SERF1 (dashed line) from Schmidtke et al. /4/.

Figure 6 shows the 85 - 90 nm emissions in all panels from each spectrometer and different channels. The scales and symbol notation are the same as Figure 5. In Figure 6*a* the 85 - 90 nm emission (ASSI A channel 12) saw a 17% rise in the model and a 27% rise in the data from day 119 to day 316 (19 data points). Figure 6*b* shows the 85 - 90 nm emission (ASSI B channel 16) with an 18% rise in the model and a 28% rise in the data from day 119 to day 316 (38 data points). Figure 6*c* shows the 85 - 90 nm emission (ASSI A channel 18) with a 16% rise in the model and a 28% rise in the data from day 119 to day 316 (20 data points). The absolute flux for all three observed time series is slightly greater than the model but well within the +35% uncertainty level as denoted by the day 315 error bar.

The conclusions that can be drawn from Figure 6 are that the ASSI A channels 12 and 18 and the ASSI B channel 16 are generally calibrated for long-term instrument sensitivity changes. The rise in the data is steeper than that expected from the model although all three channels are consistent with one another.

The absolute flux of all ASSI data is tied to the calibration of the November 10, 1988 LASP rocket (Woods and Rottman /3/). The disagreements between the ASSI/rocket data and the model generally fall within the uncertainty levels of the model even though the model uses the LASP rocket as one of the datasets for its derivation.

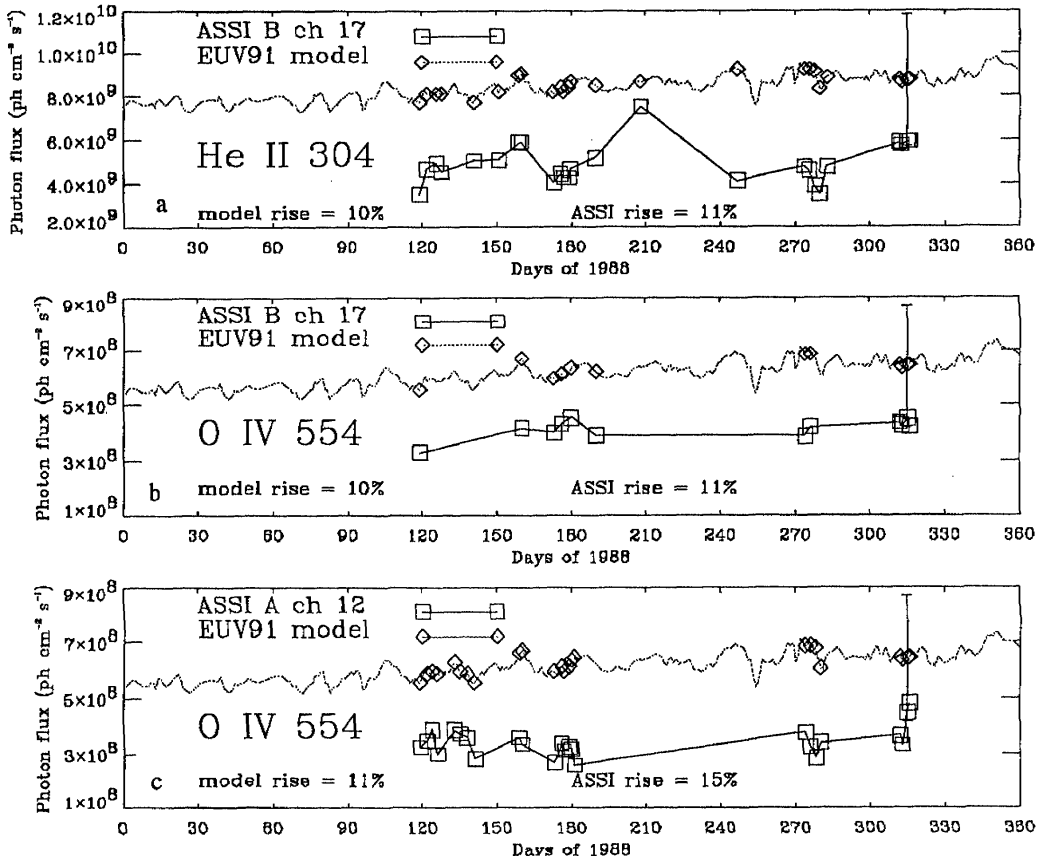

Figure 5. ASSI 30.4 (panel *a*) and 55.4 nm (panels *b* and *c*) for selected dates compared with the EUV91 model for 1988. Figure is described in text.

Four parameters have been compared to determine the internal long-term consistency of the ASSI calibration. These parameters include wavelength, date, grating, and detector/electronics. In an effort to limit the free variables, only the best solar pointing days were used in which the instrument sun-pointing system was able to minimize sun pointing misalignment. The range of values of pointing misalignment ($\Delta\alpha$), a topic to be treated in more depth in a subsequent paper, was between +0°.30 and -1°.44 for all comparisons between the four parameters where 11 to 25 days were used for each comparison dataset. In addition, only wavelengths or intervals were selected which represented emissions from the solar chromosphere, i.e., 85-90, 55.4, and 30.4 nm, in the expectation that these solar irradiances vary similarly with time. Hence, in the following comparisons, the differences are due to the four separate parameters and not to differences in solar pointing nor in physical characteristics of the solar emissions.

Figure 7, panels *a* through *i*, show the relationships between these four parameters. The difference solely between detector/electronics can be seen in Figure 7*a* where the wavelength interval (85 - 90 nm), dates of comparison (16 total), and grating (in ASSI A) are all the same. Here there is a ±6% relative uncertainty in the data. This minimum uncertainty level based on detector/electronic differences (channel 18 versus channel 12) suggests high confidence in internal long-term calibration consistency between these detectors.

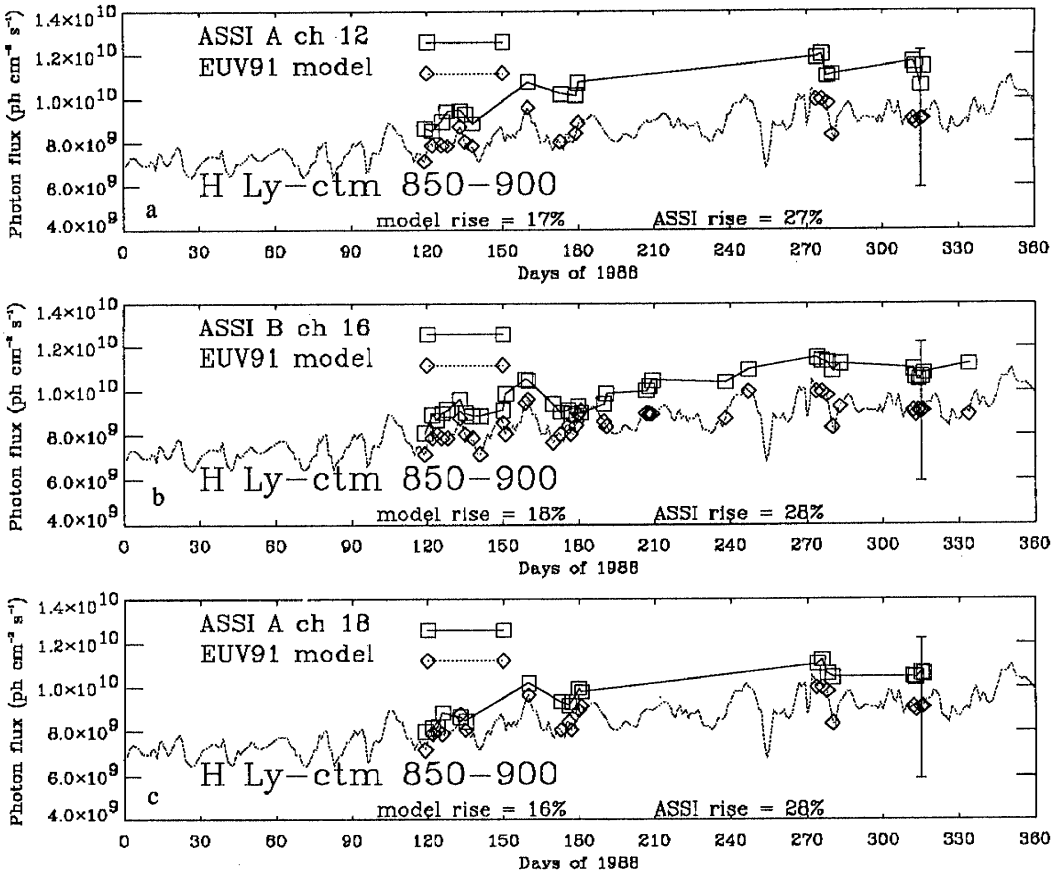

Figure 6. ASSI 85 - 90 nm (panels *a*, *b* and *c*) for selected dates compared with the EUV91 model for 1988. Figure is described in text.

In Figure 7*b* the wavelength interval (85 - 90 nm) and dates of comparison (20) are all same. There is a ±10% relative uncertainty in the data by adding grating differences (ASSI B versus ASSI A) to the detector/electronics differences (channel 16 versus channel 18). A similar comparison is made for Figure 7*c* where the wavelength interval (85 - 90 nm) and dates of comparison (19) are the same. There is a ±9% relative uncertainty in the data by adding grating differences (ASSI B versus ASSI A) to the detector/electronics differences (channel 16 versus channel 12). However, if one looks at Figure 7*d* for a different wavelength (55.4 nm) with the same dates of comparison (11), there is a ±24% relative uncertainty in the data by adding grating differences (ASSI B versus ASSI A) to the detector/electronics differences (channel 17 versus channel 12). Thus, one can summarize that there is internal long-term calibration consistency between detectors and gratings for the longer wavelength channels (ASSI B channel 16 with ASSI A channel 18) but there is not yet internal calibration consistency between detectors and gratings for the shorter wavelength channels (ASSI B channel 17 with ASSI A channel 12).

In Figure 7*e* different wavelengths are selected (55.4 and 30.4 nm) while maintaining the same dates of comparison (12), the same grating (ASSI B), and the same detector/electronics (channel 17). There is a ±20% relative uncertainty in the data from the wavelength differences. A similar comparison is made in Figure 7*f* for different wavelengths selected (85-90 and 55.4 nm) while

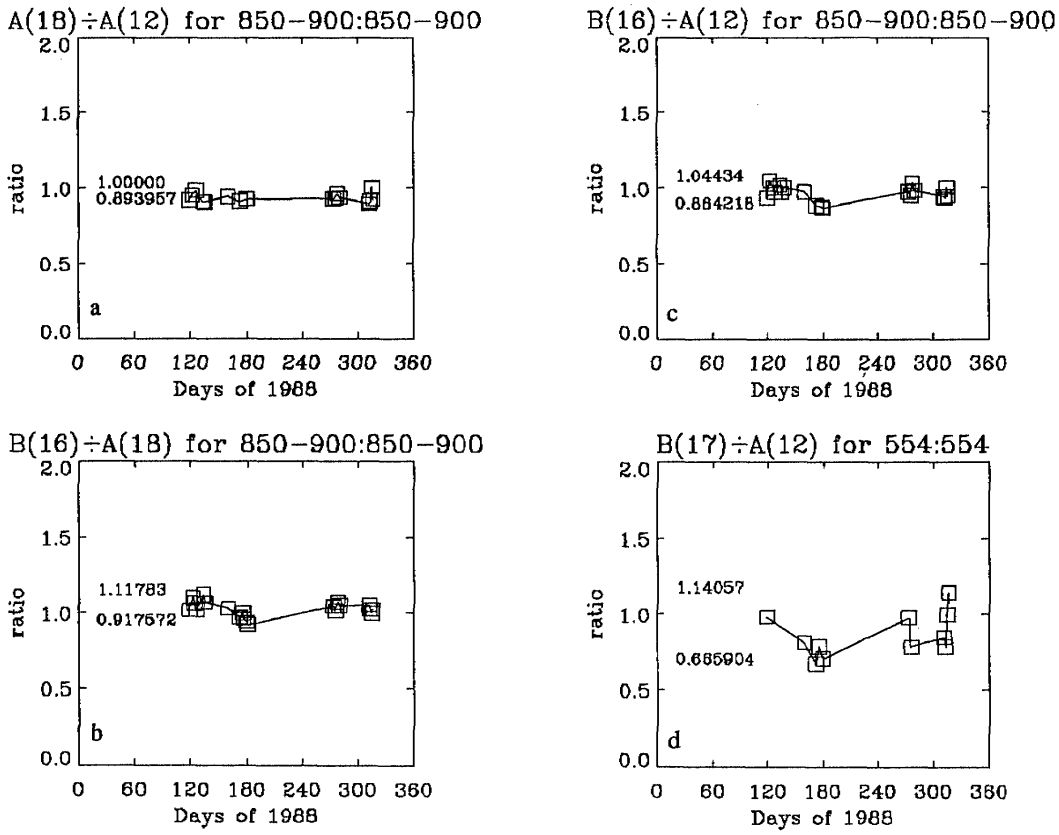

Figure 7. Panels *a* through *d* show the simple ratios of ASSI data which compare deviations from the expected ratio of 1 (i.e., no differences). The comparisons for wavelengths, dates of observations, gratings, and detectors/electronics are described in the text. Maximum and minimum ratios are shown in each panel.

maintaining the same dates of comparison (18), the same grating (ASSI A), and the same detector/electronics (channel 12). There is a ±17% relative uncertainty in the data from the wavelength differences. The conclusion drawn is that there is still uncertainty in calibrating the ASSI datasets with respect to the broad spectral interval of each channel. Whether or not this is a wavelength dependent grating, detector sensitivity, or some other calibration change over time is still an open question. An interesting bit of additional information can be obtained, however, by looking at differences across broad spectral regions between different detectors.

In Figure 7*g* different wavelengths (85-90 and 55.4 nm) and detectors (ASSI B channels 16 and 17) are selected while maintaining the same dates of comparison (12) and the same grating (ASSI B). There is a ±19% relative uncertainty in the data from the combined long to moderate wavelength and detector differences. A similar comparison is made in Figure 7*h* for different wavelengths (85-90 and 30.4 nm) and detectors (ASSI B channels 16 and 17) while maintaining the same dates of comparison (25) and the same grating (ASSI B). There is a ±49% relative uncertainty in the data from the combined long to short wavelength and detector differences. A third comparison is made in Figure 7*i* for different wavelengths (85-90 and 55.4 nm) and detec-

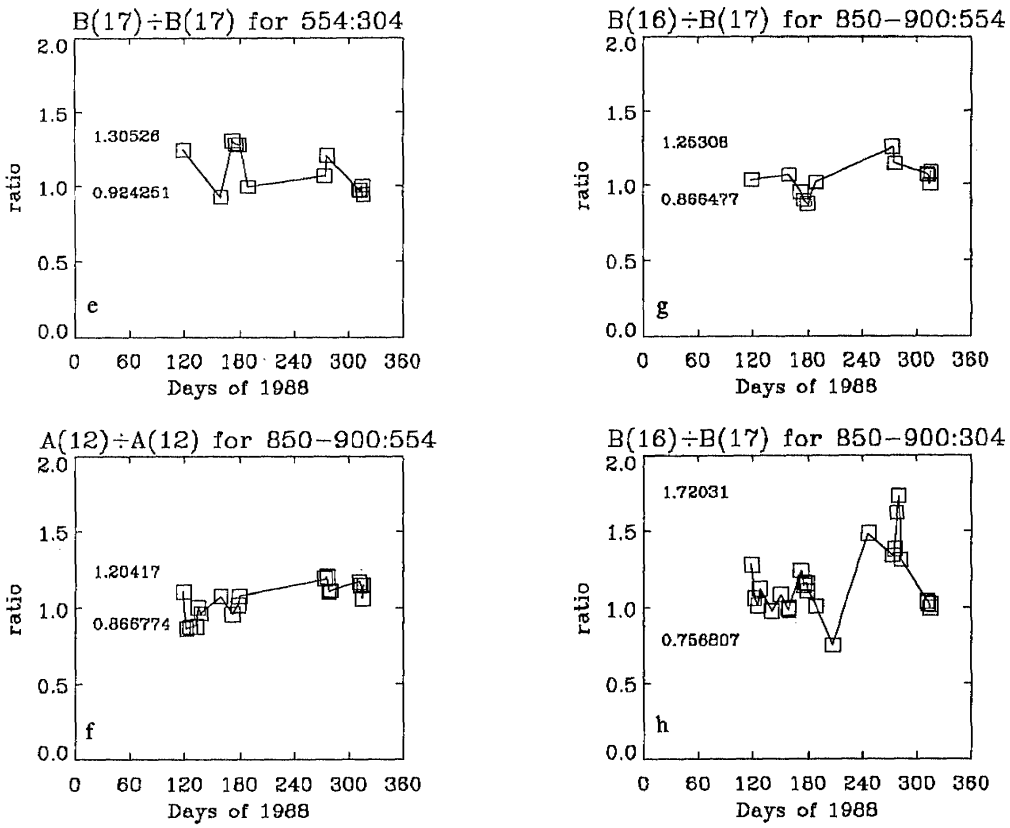

Figure 7. Panels *e* through *h* show the simple ratios of ASSI data which compare deviations from the expected ratio of 1 (i.e., no differences). The comparisons for wavelengths, dates of observations, gratings, and detectors/electronics are described in the text. Maximum and minimum ratios are shown in each panel.

tors (ASSI A channels 18 and 12) while maintaining the same dates of comparison (20) and the same grating (ASSI A). In this case, there is a ±36% relative uncertainty in the data from the combined long to moderate wavelength and detector differences. The conclusion that can be drawn from this comparison is that there in fact may be wavelength dependent grating sensitivity change over time, particularly in the grating on ASSI A, on the order of ±30% (or more with broader spectral span) since one might expect only a ±6% change due to different detectors alone, e.g., ASSI A in Figure 7*a*. A mechanism for such a long-term grating sensitivity change with wavelength is not known.

SUMMARY

ASSI B channel 17 (30.4 and 55.4 nm emissions) and ASSI A channel 12 (55.4 nm emission) are well calibrated and self-consistent in terms of long-term instrument sensitivity changes. The rise in flux levels over a half year are consistent with the rise of solar cycle 22 emission suggested by the model. ASSI A channels 12 and 18 and the ASSI B channel 16 (all 85 - 90 nm) are generally calibrated for long-term instrument sensitivity changes. The rise in the data is steeper than that expected from the model although all three channels are self consistent. The absolute flux of all ASSI data is tied to the calibration of the November 10, 1988 LASP rocket

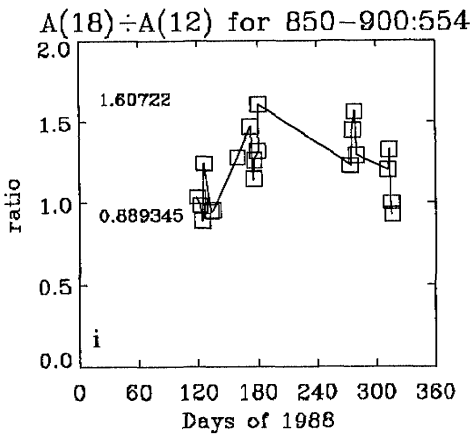

Figure 7. Panel *i* shows the simple ratios of ASSI data which compare deviations from the expected ratio of 1 (i.e., no differences). The comparisons for wavelengths, dates of observations, gratings, and detectors/electronics are described in the text. Maximum and minimum ratios are shown in each panel.

and disagreements with the EUV91 model generally fall within the latter's ±35% uncertainty levels.

Most of the uncertainty in the variations of the data can be accounted for to first order by variability within and between the four parameters of wavelength, date of observation, grating, and detector/electronics. Differences in the datasets are not due to solar pointing nor to physical characteristics of the solar emissions. There is a ±6% relative uncertainty in the data based on detector/electronic differences in ASSI A channel 18 versus channel 12 which suggests high confidence in the internal calibration consistency between these detectors. There is also internal long-term calibration consistency between detectors and gratings for the longer wavelength channels (ASSI B channel 16 and ASSI A channel 18) but there does not yet seem to be internal long-term calibration consistency between detectors and gratings for the shorter wavelength channels (ASSI B channel 17 and ASSI A channel 12). There is also uncertainty in calibrating the ASSI datasets with respect to the broad spectral interval over each channel. Whether or not this is a wavelength dependent grating or detector sensitivity change over time remains an open question although it is possible there may beunexplained grating changes.

There are additional remaining calibration issues which have also not been resolved. For example, solar pointing analysis which takes into account the percent of the entrance slit projected onto a grating will correct some of the day-to-day variation and make more data available for study. It was noted that there are some discrepancies at shorter wavelengths between the EUV91 model and LASP rocket data. These can be resolved by more observations during moderate solar activity. The resolution of this issue would affect 30.4 and 55.4 nm absolute flux values in particular. It may also be interesting to revisit the long-term detector degradation curves for the 85 - 90 nm wavelengths based upon the expected solar cycle rise as shown by EUV91.

ACKNOWLEDGMENTS

This research was supported through the NATO grant CRG 910461 and NASA grant NAG5-665. Publication assistance was provided through TELOS Systems Group.

REFERENCES

1. Schmidtke, G., P. Seidl, and C. Wita, Airglow-solar spectrometer instrument (20-700 nm) aboard the San Marco D/L satellite, *Appl. Op.*, **24**, 3206-3213 (1985).

2. Schmidtke, G., H. Doll, and C. Wita, Measurement of solar EUV/UV radiation of the steeply rising solar cycle 22 during the San Marco-5 mission and proposed instrumentation to achieve high radiometric accuracy, *Adv. Space Res.*, **13**, in press (1993).

3. Woods, T.N. and G.R. Rottman, Solar EUV irradiance derived from a sounding rocket experiment on November 10, 1988, *J. Geophys. Res.*, **95**, 6227-6236 (1990).

4. Schmidtke, G., T. Woods, H. Doll, J. Worden, S.C. Solomon, C. Wita, and G. Rottman, Solar EUV irradiance from the San Marco ASSI: a reference spectrum, *Geophys. Res. Lett.*, in press (1992).

5. Tobiska, W.K., Revised solar extreme ultraviolet flux model, *J. Atmos. Terr. Phys.*, **53**, 1005-1018 (1991).

6. Tobiska, W.K., S. Chakrabarti, G. Schmidtke, and H. Doll, Comparative solar EUV flux for the San Marco ASSI, *Adv. Space Res.*, **13**, 255-259 (1993).

7. Schmidtke, G., H. Doll, C. Wita, and S. Chakrabarti, Solar EUV/UV and equatorial airglow measurements from San Marco-5, *J. Atmos. Terr. Phys.*, **53**, 781-785 (1991).

8. Ogawa, H.S., L.R. Canfield, D. McMullin, and D.L. Judge, Sounding rocket measurement of the absolute solar EUV flux utilizing a silicon photodiode, *J. Geophys. Res.*, **95**, 4291-4295 (1990).

9. Donnelly, R.F. and J.H. Pope, The 1-3000 Å solar flux for a moderate level of solar activity for use in modeling the ionosphere and upper atmosphere, *NOAA Technical Report ERL 276-SEL 25*, Boulder (1973).

10. Hinteregger, H.E., K. Fukui, and B.R. Gilson, Observational, reference and model data on solar EUV, from measurements on AE-E, *Geophys. Res. Lett.*, **8**, 1147-1150 (1981).

11. Schmidtke. G., EUV indices for solar-terrestrial relations, *Geophys. Res. Lett.*, **3**, 573-576 (1976).